

The observation of “conduction spot” on NiO resistance RAM

Takashi Fujii¹, Hirofumi Kondo¹, Hiromichi Kaji¹, Masashi Arita¹, Masahiro Moniwa²,
Takeshi Yamaguchi², Ichiro Fujiwara², Masaki Yoshimaru², and Yasuo Takahashi¹

¹ Graduate School of Information Science and Technology, Hokkaido University, Sapporo, 060-0814, Japan

Tel: +81-011-706-6457 E-mail: t-fujii@ist.hokudai.ac.jp

² Semiconductor Technology Academic Research Center, 3-17-2 Shinyokohama, Kohoku-ku, Yokohama, 222-0033, Japan

1. Introduction

Resistance random access memories (ReRAMs) have attracted much attention because of the superior scalability related to its simple Metal/Oxide/Metal (MOM) structure [1, 2, 3]. In these years, various binary oxides have been reported, such as NiO etc. to show the resistance switching (RS). Prior to the operation, the MOM structure should be set in the low resistance state (LRS) by applying relatively high voltage, *e.g.* more than 5V. This is the forming process. Afterwards, it was in the high resistance state (HRS) by relatively low voltage, *e.g.* around 1 V. (reset process, RESET). Finally by intermediate voltage, *e.g.* around 2V, this HRS changed to LRS again (set process, SET). To understand this RS mechanism, a filament-model has been proposed [4, 5]. Although the mechanism is still obscure, based on this model, a filament-like local area in LRS appears during the forming process. In this work, we call this area as a “conduction spot” (CS). The filament-like conduction path is disconnected and connected in RESET and SET processes, respectively.

CS is the region where RS occurs, and therefore the forming process has a key to understand RS and to control ReRAM properties. In this work, we observed CSs in NiO ReRAM in detail by means of *in-situ* optical microscopy (OM), SEM as well as TEM. Energy dispersive X-ray spectroscopy (EDX) was employed to reveal the filament path. The size of CS which may relate to ReRAM scaling law was controllable by electric power introduced during the forming process.

2. Device Fabrication and I-V Characteristics

Fabricated NiO ReRAM has a simple MOM structure on a SiO₂/Si (100) substrate (Fig. 1), which was deposited by radio frequency (RF) sputtering at room temperature (RT). First, we formed a 100-nm thick Pt bottom electrode (BE) on a Ti adhesion layer. Next, a 100nm thick Ni film was deposited. To obtain NiO, it was oxidized in air for 3 min. at 500-800°C (T_0). Finally, Pt top electrodes (TE) were formed from 50- μ m to 1-mm square, 50-nm thick. Clear non-polar I-V hysteresis was achieved (Fig. 2(a)), when we set a current compliance in measurement system during the forming and SET processes. Typically, we attached a resistor to a ReRAM cell in series for proper control of current limitation (Fig. 2(b)), where injection power reached maximum just after the forming.

3. Effects of Oxidation Temperature

The NiO formation was checked by XPS (X-ray photoelectron spectroscopy) analysis. Ni layer was fully oxidized at the temperature higher than $T_0 = 600^\circ\text{C}$ (Fig. 3). The forming voltage (V_F) tends to be higher as T_0 increases (Fig. 4). The interesting point is that the V_F were scattered from one device to another as T_0 increases, and the scattering width of the V_F became wider in the small TEs. These phenomena may be due to the existence of weak spots against forming related to random nature of forming. But, initial resistances (HRS) clearly increased as T_0 increase (Fig. 5). These results can be understood that high temperature oxidation improve the crystallinity and decreases the number of weak spots of NiO films, thus V_F was scattered heavily. We exploited the phenomena to observe CS. When we form NiO at 800°C, extra high power were concentrated in small weak spot, which smash the TE and enables us to detect the CS.

4. Conduction Spot

By adequate selection of T_0 of 800°C, we can successfully increase V_F and thus the injection power, which makes CS visible on OM. In OM images (Fig. 6), a black dot (circle) corresponding to CS is recognized in the upper part of TE after forming while there was no trace before forming. To confirm this dot corresponds to CS, firstly, we cut the device into two pieces and performed a forming treatment to the lower half in HRS (Fig. 7). The 2nd dot appeared in addition to the 1st dot. By cutting again into left and right parts, the 3rd dot appeared. Forming voltage increased step by step (Fig. 8). The weakest spot in the oxide film must selectively contribute to CS.

The SEM image of CS and corresponding TEM image (Fig. 9) show that a through hole was generated in the Pt TE. NiO was melted and recrystallized. Although these images suggest some kind of breakdown (BD), it was not permanent BD because reproducible RS was observed over 50 cycles after CS was generated (Fig. 10). To get information about the local area, the CS edge was investigated by EDX (Fig.9(c)). The triangles far from this edge showed the composition of Ni:O \approx 1:1. On the other hand, the compositions of the region indicated by red circles and yellow squares at the edge were Ni:O \approx 9:1 and 2:1 respectively, indicating the existence of oxygen defective NiO. This area may play as the filament path giving the ReRAM switching phenomenon. This device was HRS, therefore the filament path was discontinuous.

For stable operation of ReRAM, CS area must be controlled. We investigated the influence of current compliance on CS area (Fig. 11). It became smaller by the strong current limitation. The CS area defined the area of a crater shows a clear dependence on the maximum injection power at the forming (Fig. 12). This dependence shows the roadmap of ReRAM scaling, for example, the device size can be diminished to less than 100 nm by realizing the forming power of 10⁻⁵ W. Note that we actually found many conductive small areas in the crater by the use of conductive AFM (Fig. 11(f)).

5. Conclusion

We succeeded to identify CS which is the platform of filamentary conduction in a NiO based ReRAM prepared at 800°C. Probably CS appears at a “weak spot” by forming. The EDX analysis in CS suggests the filament formation, and further careful analysis will reveal the chemical composition of the filament. The results in this work suggest that the potential of scalability on ReRAM is determined by the forming power. To reduce this power, an exact current compliance method should be used. In addition, both high initial state and low forming voltage have to be realized.

Acknowledgements: The authors thank Drs. Masaki Aoki, Toshio Kobayashi, and Yoshinori Maeno for helpful discussion. The work is partly supported by a Grant-in-Aid from JSPS as well as MEXT (20035001 and 2156081).

References

- [1] I. G. Baek *et al.*, IEDM Tech. Dig., p.587, 2004.
- [2] K. Tsunoda *et al.*, IEDM Tech. Dig. p767, 2007.
- [3] B. Lee and H.-S. P. Wong VLSI Tech. 2B-4, 2009.
- [4] C. Cagli *et al.*, IEDM Tech. Dig. p.301, 2008.
- [5] K. Kinoshita *et al.*, Appl. Phys. Lett. 89, 103509, 2006

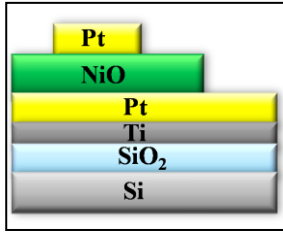


Fig.1 Schematic drawing of NiO MOM structure.

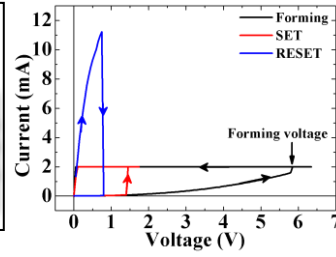


Fig.2 (a) Typical DC I-V characteristics with current compliance set by a voltage source. (b) The I-V characteristics (black curve) and the power (red curve) in the forming process with a load resistor of 100 k Ω .

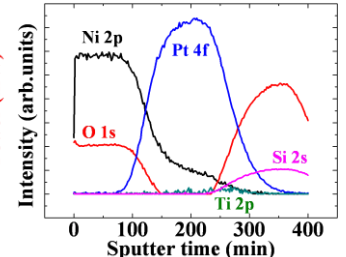
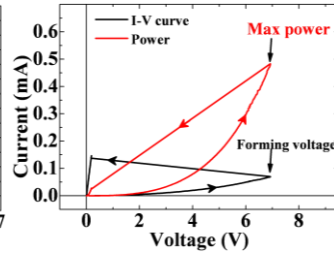


Fig.3 XPS depth profile of the device oxidized at 600°C.

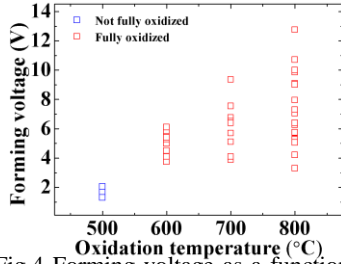


Fig.4 Forming voltage as a function of oxidation temperature. The Ni layer was fully oxidized over 600°C.

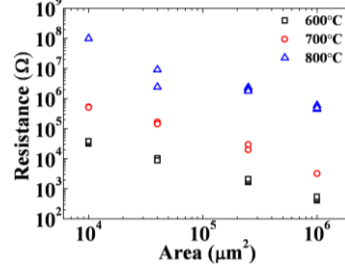


Fig.5 Initial resistance as a function of TE area for the NiO films oxidized at 600, 700, 800°C.

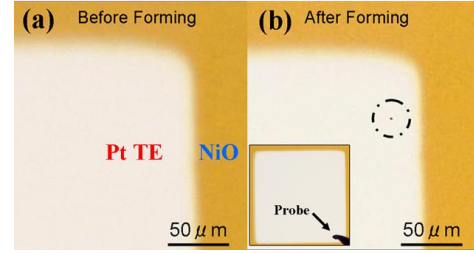


Fig.6 Optical micrographs of a top electrode (a) before and (b) after forming. CS (black dot in a circle) was seen only in (b). Inset: overall image of the electrode (500 μ m square) indicating CS and probe positions.

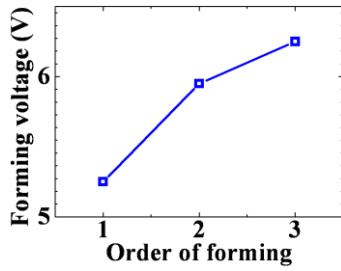


Fig.8 Forming voltage of the 1st, 2nd and 3rd forming.

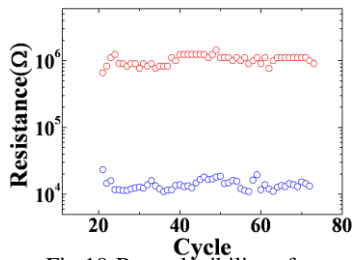


Fig.10 Reproducibility of over 50 cycles after CS was generated.

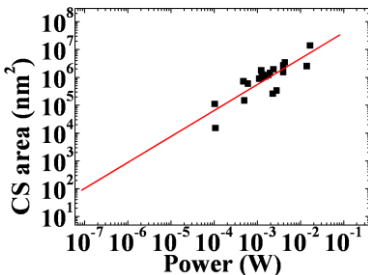


Fig.12 CS area as a function of injected maximum power (current \times voltage) at the forming. It is proportional to the power.

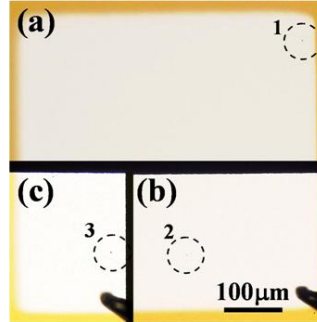


Fig.7 Optical micrographs after (a) the 1st forming (b) the 2nd forming after cutting device and (c) the 3rd forming after the next cut. Separated device before forming included no CS.

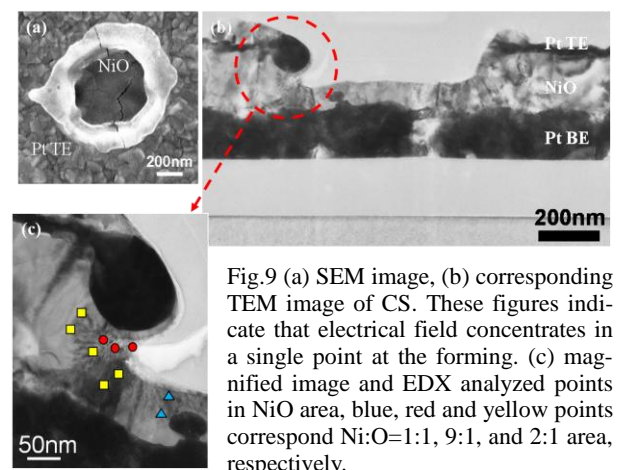


Fig.9 (a) SEM image, (b) corresponding TEM image of CS. These figures indicate that electrical field concentrates in a single point at the forming. (c) magnified image and EDX analyzed points in NiO area, blue, red and yellow points correspond Ni:O=1:1, 9:1, and 2:1 area, respectively.

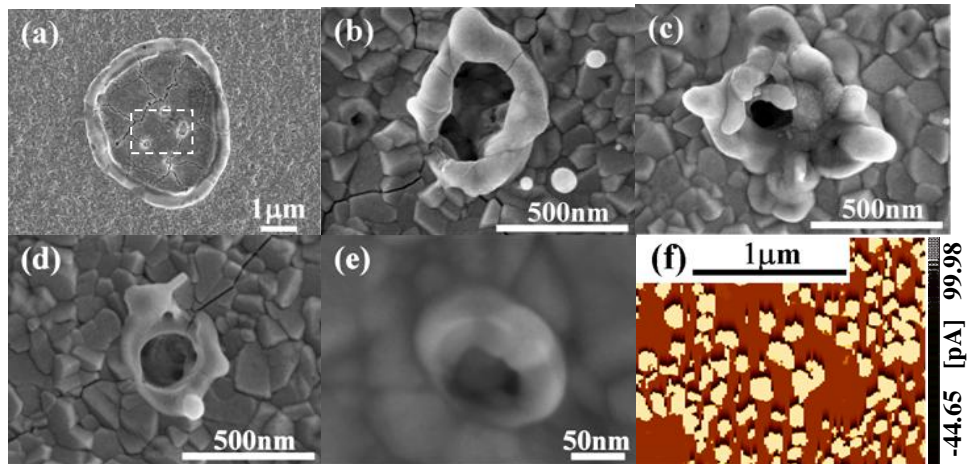


Fig.11 SEM image of CS area controlled by injection power with respective current compliance (a) 2 mA (set by the voltage source), (b) 10 k Ω , (c) 20 k Ω , (d) 100 k Ω , (e) 470 k Ω (f) conductive AFM image from the center of the crater formed by 2 mA (enlarged area shown by square in (a)).